Supplementary methods

Biomarker extractions and GC-MS quantification

The biomarker extraction and analysis were conducted as the following procedure. In the process of solvent extraction, ~1 g of soil was extracted three times with 20 ml extraction solution (dichloromethane:methanol = 1:1; v/v) by 15 min of ultrasonication. The combined extracts were then filtered through glass fiber columns and concentrated by rotary evaporation, and finally dried with N_2 gas in 2 mL glass vials.

For hydrolysable lipid extraction, we added 15 mL of methanolic KOH (1 M) and 0.4 g air-dried soil residues (after the solvent extraction) into teflon-lined bombs to ensure seal, and heated at 100 °C for 3 h. After cooling, the extracts were acidified to pH 1 with HCl (6 M). Hydrolysable lipids were then obtained by liquid-liquid extraction with 20 mL ethyl acetate three times, concentrated by rotary evaporation, and dried with N_2 gas. The extracts were methylated with 14% diazomethane (reaction for 90 min at 70 ^{o}C), recovered by liquid-liquid extraction with hexane three times, and dried with N_2 gas.

For lignin-derived phenol analysis, 0.3 g soil residues (after the solvent extraction), 1 g CuO and 100 mg ammonium iron (II) sulfate hexahydrate, and 15 ml of NaOH (2 M) were added in teflon bombs and then heated at 170 °C for 2.5 h. The extracts were acidified to pH 1 with HCl (6 M) and kept at room temperature for 1 h in the dark.

After centrifuging at 3000 rpm for 15 min, the supernatant was transferred to a funnel and recovered by liquid-liquid extraction with 20 mL ethyl acetate three times. The ethyl acetate extracts were then concentrated by rotary evaporation and dried under N_2 gas.

Extracts from all three processes (solvent extraction, base hydrolysis, and CuO oxidation) were derived with trimethylsilyl (TMS) by reaction with 100 μl N,O-bis-(trimethylsilyl) trifluoroacetamide (BSTFA) and 50 μl pyridine at 60 °C for 2 h. The biomarkers were analyzed on a gas chromatography-mass spectrometry (GC-MS; Agilent 7890A-5973N, Palo Alto, USA) with a flame ionization detector (FID) to quantify biomarkers. Data were acquired and processed with GC ChemStation (Rev. B.04.02) software. The concentration of individual compounds was quantified through external standards and normalized to the sample SOC concentration.

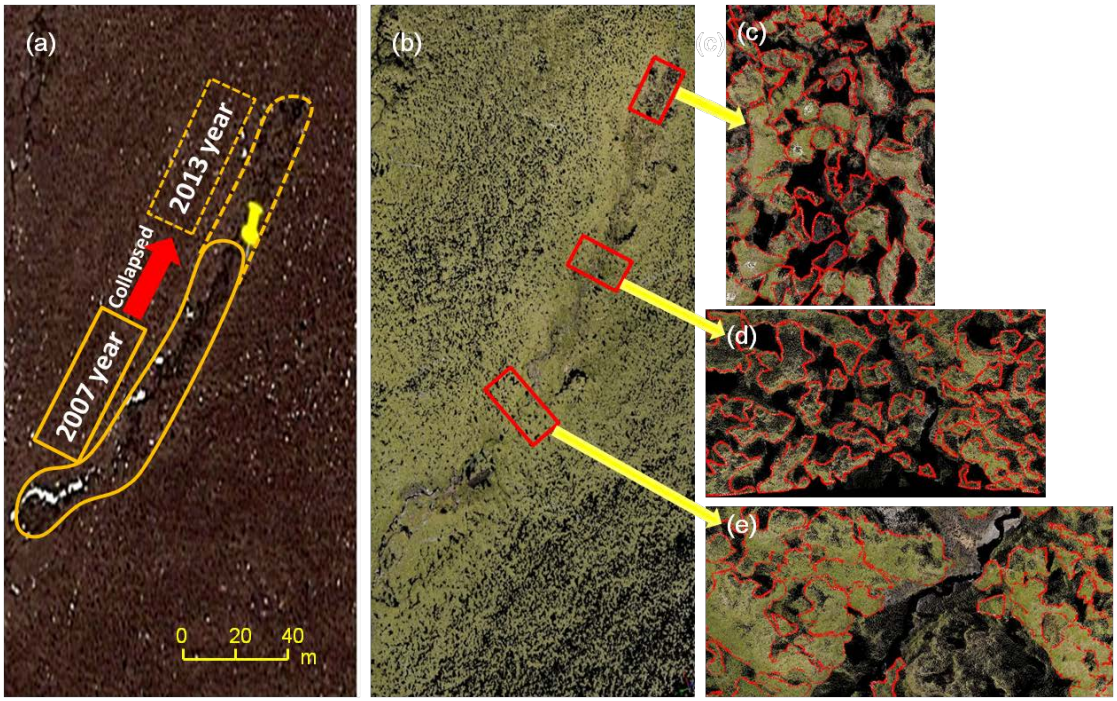

Figure S1 Satellite image of an upland abrupt thaw feature on the Tibetan Plateau obtained from Google Earth (a), the image captured from coloured LiDAR point cloud data for the upland thaw feature (b), and amplified images captured from LiDAR data for the three plots within the feature, in which many patches of vegetation and exposed soil are observed (c-e). The solid line in panel (a) indicates the shape of the abrupt thaw feature in 2007, and the dashed line represents the retreat outline of the landscape six years later. The three red rectangles in panel (b) indicate the specific positions of three collapse plots in different years (1, 10, 16 years) since collapse in the landscape. Red polygons in panels (c-e) describe the shape of the vegetated patches along three transects.

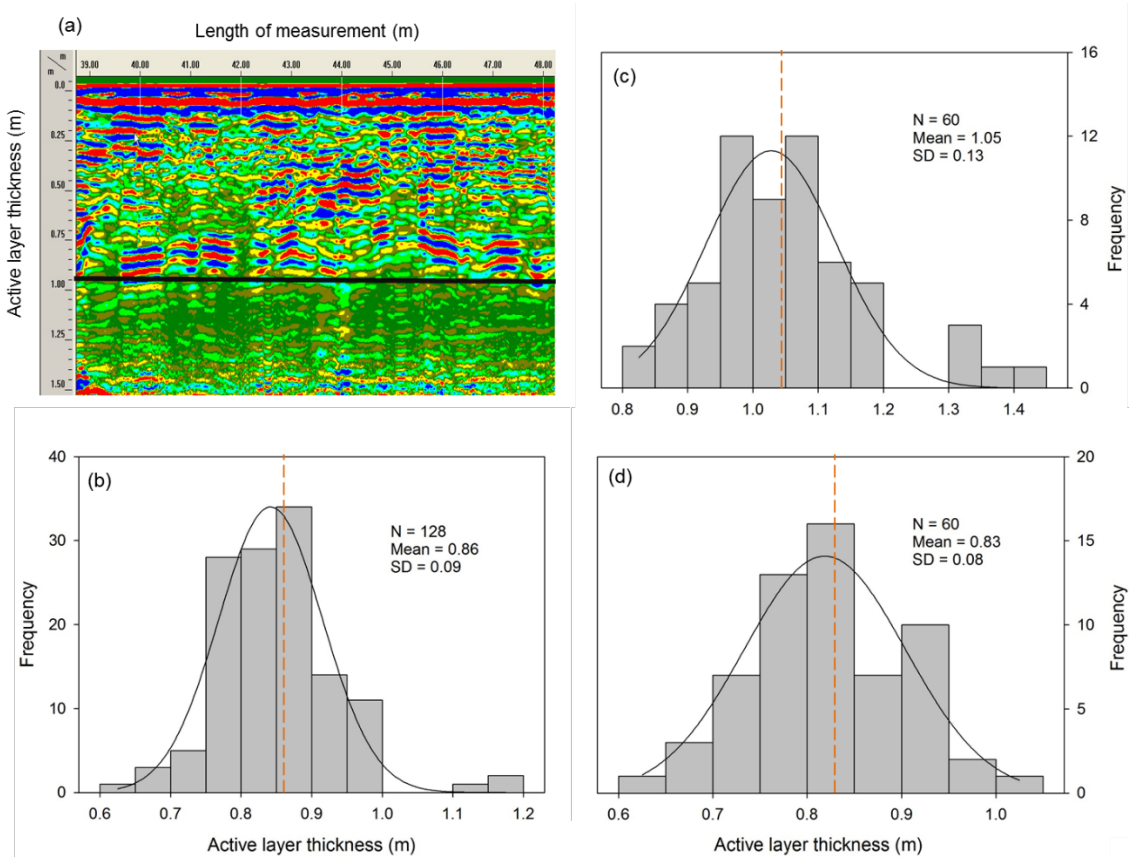

Figure S2 Active layer thickness (ALT) of the experimental site measured using georadar (a) and a steel probe (b-d). Panels (a, b) show the ALT data measured across the overall study area, while panels (c, d) indicate the ALT within and outside the thaw feature, respectively. The black line in panel (a) shows the depth where existing strong radar reflection between the unfrozen soil and permafrost, which separates the active layer from the permafrost. Different colours in panel (a) represent the different materials' radar reflections. The orange dashed line in panels (b-d) represents the mean value of ALT.

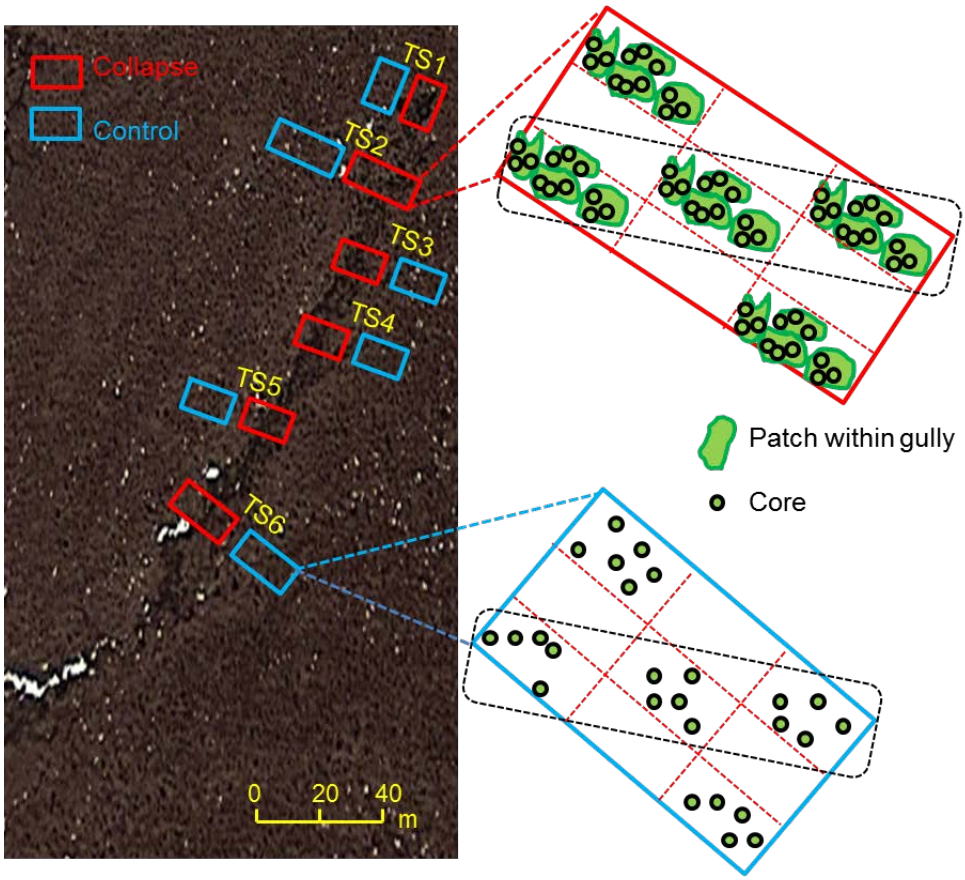

Figure S3 Schematic diagram of soil sampling in the studied thaw feature in the upland region of the Tibetan Plateau. The specific positions of six sampling transects (TS1-TS6) are marked in the diagram. Red and blue rectangles represent the collapse plots and control plots along six transects, respectively. Specifically, both collapse and control plots were divided into nine equal grid cells. All the soil samples were then assigned to one of these 9 grid cells according to the location of each patch. Only soil samples within the three diagonal grid cells were selected and mixed separately to obtain three replicate samples.

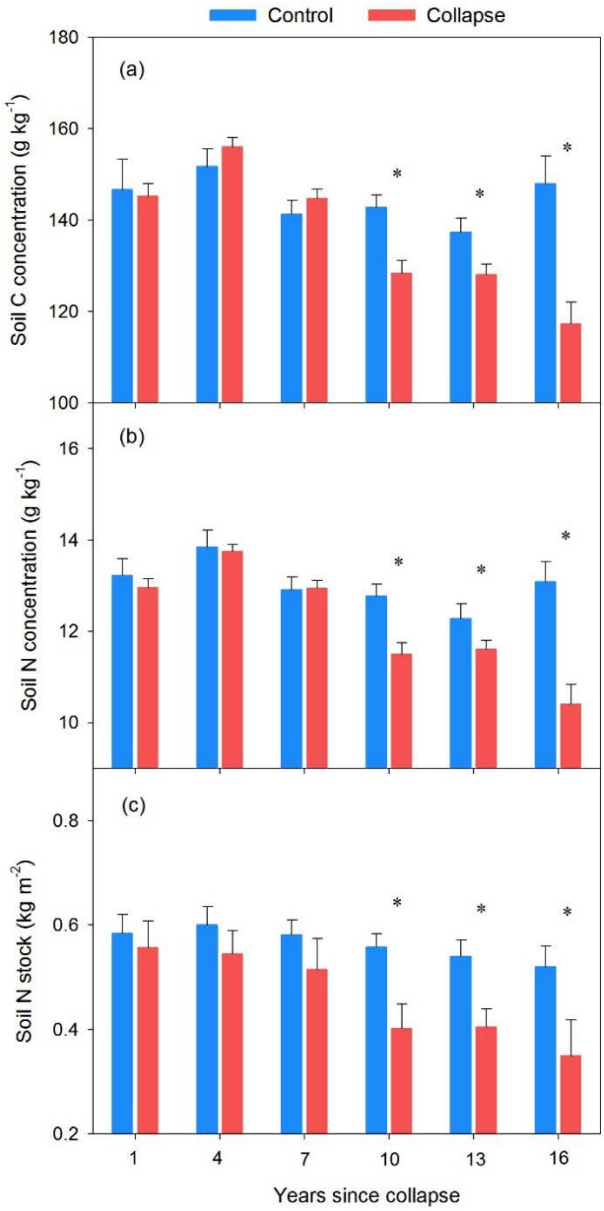

Figure S4 Comparisons of (a) soil carbon (C) concentration, (b) nitrogen (N) concentration and (c) N stock between collapse (red) and control (blue) plots in different years since permafrost collapse. Notably, as the control plots (blue) were paired with the collapse plots (red), the variations of C concentration, N concentration and stock in the control plots along the thaw sequence were due to spatial variability rather than abrupt thaw effects. Significant differences between collapse and control plots are denoted by an asterisk (*) ($P < 0.05$).

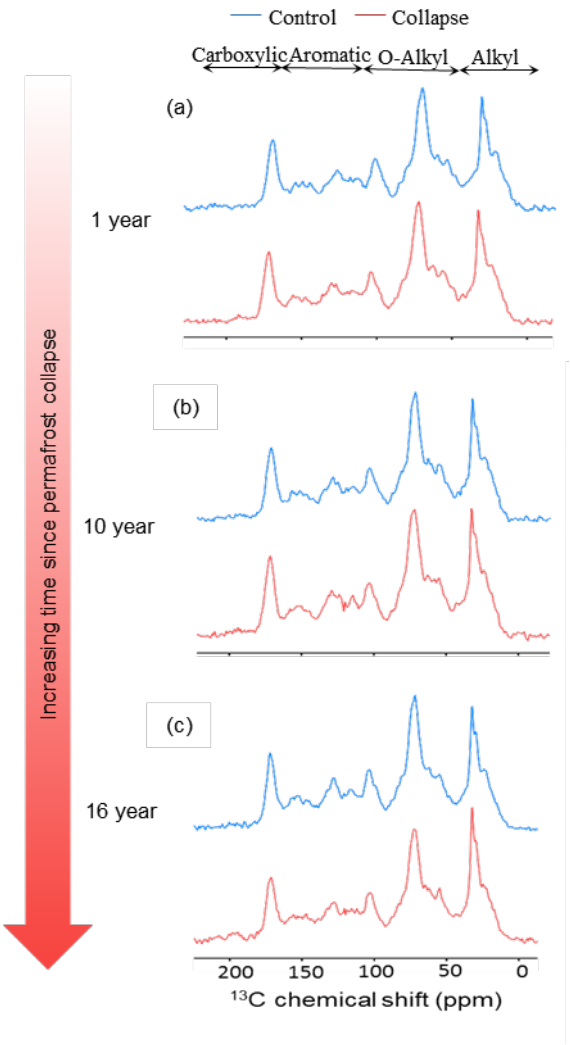

Figure S5 Comparisons of ^{13}C NMR spectra between collapse (red) and control (blue) plots in different years since permafrost collapse. Subpanels (a-c) correspond to the ^{13}C NMR spectra of soil organic matter (SOM) derived from samples of soil collapsed for 1 year, 10 years and 16 years, respectively. The chemical shift regions 0-50, 50-110, 110-165, and 165-215 ppm refer to alkyl C, O-alkyl C, aromatic C and carboxylic C, respectively (Simpson and Simpson 2012).

Table S1 Characteristics of six collapse plots along a thaw sequence on the Tibetan Plateau.

Years since collapse	Plot area (m^2)	Groundcover within features (%)		Patch quantities	Dominant species
	Length × width	Vegetated patch	Exposed soil		
1	15 m × 10 m	89	11	32	*Kobresia tibetica*, *K. royleana*, *Carex atrofusca*
3	30 m × 10 m	90	10	43	*K. tibetica*, *K. royleana*, *C. atrofusca*
7	15 m × 10 m	78	22	30	*K. tibetica*, *K. royleana*, *C. atrofusca*
10	15 m × 10 m	74	26	30	*K. tibetica*, *K. royleana*, *C. atrofusca*
13	15 m × 10 m	74	26	27	*K. tibetica*, *K. royleana*, *C. atrofusca*
16	20 m × 10 m	65	35	25	*K. tibetica*, *K. royleana*, *C. atrofusca*

Table S2 Chemical composition of soil samples collected along a thaw sequence on the Tibetan Plateau.

Years since collapse	Plot	Solvent-extractable compounds (mg g^{-1} C)	Hydrolysable lipids (mg g^{-1} C)		Lignin-derived phenols (mg g^{-1} C)		
		Carbohydrates	Cutin-derived compounds	Suberin-derived compounds	Vanillyls	Syringyls	Cinnamyls
1	Control	0.37 (0.03)	2.93 (0.25)	2.42 (0.11)	5.46 (0.24)	5.36 (0.27)	8.61(0.26)
	Collapse	0.29 (0.11)	2.57(0.13)	3.18 (0.38)	5.36 (0.04)	5.07 (0.07)	7.23 (0.17)*
10	Control	0.45 (0.14)	2.64 (0.36)	3.14 (0.12)	5.21 (0.22)	4.75 (0.29)	8.31 (0.59)
	Collapse	0.37 (0.04)	2.42 (0.12)	3.23 (0.32)	6.18 (0.20)	5.84 (0.12)	7.69 (0.32)
16	Control	0.62 (0.10)	2.64 (0.24)	2.71 (0.09)	5.66 (0.24)	5.01 (0.23)	8.86 (0.47)
	Collapse	0.31 (0.03)*	2.51 (0.21)	3.49 (0.17)*	6.80 (0.18)*	6.33 (0.12)*	9.38 (0.23)

Cutin-derived compounds including mid-chain hydroxy C_{14}, C_{15}, C_{17} acids + C_{16} mono- and dihydroxy acids and diacids; Suberin-derived compounds including ω-hydroxyalkanoic acids C_{20}-C_{32} + α, ω-diacids C_{20}-C_{32}. Standard errors are presented in parentheses (n = 3). Significant differences between collapse and control plot are denoted by an asterisk (*) ($P < 0.05$).

Table S3 Degradation parameters of lignin-derived phenols and cutin-derived compounds along a thaw sequence on the Tibetan Plateau.

Years since collapse	Plot	$(Ad/Al)_v$	$(Ad/Al)_s$	$\omega\text{-}C_{16}/\Sigma C_{16}$	$\omega\text{-}C_{18}/\Sigma C_{18}$
1	Control	0.72(0.03)	0.79(0.04)	0.39(0.01)	0.22(0.02)
	Collapse	0.70(0.01)	0.83(0.02)	0.42(0.01)	0.22(0.01)
10	Control	0.82(0.03)	1.00(0.08)	0.44(0.02)	0.23(0.03)
	Collapse	0.77(0.04)	0.97(0.07)	0.46(0.01)	0.27(0.02)
16	Control	0.78(0.05)	0.93(0.10)	0.43(0.003)	0.20(0.02)
	Collapse	0.77(0.03)	0.95(0.05)	0.47(0.01)*	0.25(0.01)*

$(Ad/Al)_v$ is the ratio of vanillic acid to vanillin; $(Ad/Al)_s$ is the ratio of syringic acid to syringaldehyde; $\omega\text{-}C_{16}/\sum C_{16}$ is the ratio of ω-hydroxy C_{16} acid to the total of ω-hydroxyalkanoic acid, n-alkane-α,ω-dioic acid, and mid-chain-substituted acids with 16 carbons; $\omega\text{-}C_{18}/\sum C_{18}$ is the ratio of ω-hydroxy C_{18} acid to the total of ω-hydroxyalkanoic acid, n-alkane-α,ω-dioic acid, and mid-chain-substituted acids with 18 carbons. Standard errors are presented in parentheses (n = 3). Significant differences between collapse and control plot are denoted by an asterisk (*) ($P < 0.05$).